IMEKO 22nd TC3, 12th TC5 and 3rd TC22 International Conferences
3 to 5 February, 2014, Cape Town, Republic of South Africa

A NON-IMAGING OPTICAL SYSTEM FOR CHARACTERISATION OF BALL-SHAPED MICRO-INDENTERS

Febo Menelao, Zhi Li, Uwe Brand, Andre. Felgner

Physikalisch-Technische Bundesanstalt, Bundesallee 100, 38116 Braunschweig, Germany, Febo.Menelao@ptb.de

Abstract: To quantitatively determine the tip radius of spherical and conical indenters, a practical non-contact radius measurement system is presented. Realization of the optical system has been detailed, including its theoretical and actual resolution and error sources. For the purpose of experimental investigation of the performance of the non-imaging radius measurement system, a sapphire sphere with a nominal radius of 200 µm has been employed. Detailed data analysis indicates that high-order form error of the object under test might be one of the key error sources within the calibration setup.

Keywords: Confocal microscopy, micro- and nanoindentation, indenter, Rockwell indenter, ball-shaped indenter, radius measurement.

1. INTRODUCTION

Hardness testing is one of the important approaches to determine the mechanical properties of materials. Nowadays, with the help of Finite Element Analysis more mechanical properties, like Young's modulus, yield strength, etc, can be interpreted from those typical indentation testing data [1-2]. The measurement uncertainty of hardness tests is, however, subject to a few factors, in which the form error of the indenter in use is always one of the significant error sources. To improve the measurement uncertainty, it is therefore strongly desired to calibrate the geometric form of indenters before being used [3-4].

Typical means for the calibration of the microform of an indenter can be classified into two types: contact and non-contact approaches. The contact-based approaches include the use of micro-coordinate measuring machines, or even a nanomeasuring machine, which features large measurement range (up to tens of mm) with nanometer resolution. However, this kind of calibration approach, in general, suffers from such shortages as time-consuming measurement procedure, difficulties in data evaluation, etc.

Non-contact form measuring systems including interference microscopes, confocal microscopes, etc., demonstrate usually high resolution and relatively easy operation, and therefore have also been applied for the calibration of various indenters. However, due to the desired large lateral measurement range (~ 200 µm x 200 µm) and large measurement depth (~ 60 µm) the overall topography of an indenter, a Rockwell indenter in particular, couldn't be directly imaged by a conventional interference or confocal optical microscope [5-6]. To obtain the 3D geometry of an indenter under test, one of the usual ways is to employ the imaging stitching technique to put together numbers of sub-region images of the indenter, which would, in return, impose high requirements to the 3D scanning system.

Recently a non-imaging optical system for characterization of ball-shaped indenters has been developed at the Physikalisch-Technische Bundesanstalt. The fundamental principle of this system is detailed in section 2. System realization is discussed in section 3. Experimental investigation of the measurement capability of the calibration setup is presented and discussed in section 4. Further development of this system is outlined in section 5.

2. PRINCIPLE

The non-imaging tip radius measuring system [7] is developed on basis of a confocal (position)-sensing method, as illustrated in Fig. 1: a monochromatic light with a plane wavefront is delivered into the optical system to illuminate the sample to be measured, yielding a focused spot on the focal plane of the objective. The reflected light coming from an object under test is collected by the same objective and then focused in the back focal plane of a tube lens, and finally detected by a point-like photo-detector.

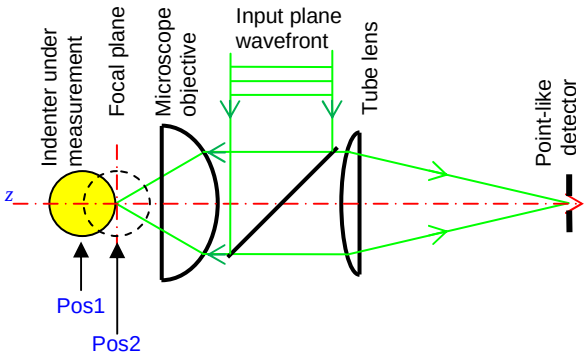

Fig. 1. Working principle of an optical non-imaging system for the determination of the tip radius of spherical indenters

For a spherical object, the maximum signal intensity would appear when

(1) the top surface of the object is in the focal plane of the microscope objective, i.e. z = Pos1, as shown in Fig. 1,

(2) the center of the sphere under test is located in the objective's focal plane, i.e. z = Pos2, as illustrated in Fig. 1.

Obviously, in the case of an ideal optical system (e.g. without lens aberration and positioning/alignment error) and an ideal sphere under test (e.g. highly reflective, no form error, fully smooth, etc.), the radius of the sphere under test can be determined by measuring the distance between Position 1 and 2.

3. OPTICAL SYSTEM, DATA EVALUATION AND MEASUREMENT ERROR ANALYSIS

There exist generally different ways to realize a tip-radius measurement system on basis of the fundamental principle shown in Fig. 1, as detailed in [7]. For the purpose of understanding the potential measurement errors of this method, here the following approaches have been employed.

3.1 Illumination and imaging system

A He-Ne Laser has been utilized as one of the light sources of the measurement system. The laser light is coupled into a single-mode fiber delivery system and then sent to the optical setup, offering a nearly-perfect point-like illumination.

The infinity-corrected microscope objective used in this system has a numerical aperture of A_N = 0.75, which is adequate for spherical/conical indenter with an apex angle no larger than 90°. In the case of measuring a flat surface or ideal sphere, the theoretical axial resolution of the optical system using this objective amounts to

$$\delta z = \frac{0.9\lambda}{A_N{}^2} = 1.0\ \mu\text{m}. \qquad (1)$$

It's worthwhile to mention that the real axial confocal resolution of the optical system using this objective is actually subject to the geometrical form of the object under test (and its spatial holding status [7]). Taken as an example, for a Rockwell indenter with its mounting axis parallel to the optical axis of the objective, the actual A_N of the objective is reduced to be 0.5, since the reflected light from the shoulder of the indenter couldn't be collected by the objective. And the axial confocal resolution of this optical system for a normally mounted Rockwell indenter is therefore decreased to 2.3 µm.

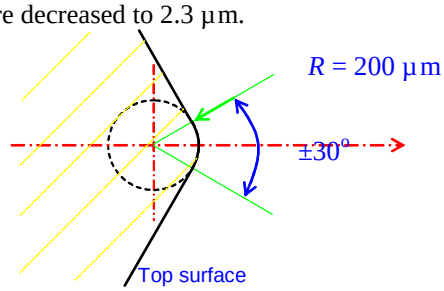

Fig. 2. Analysis of the actual axial-resolution of the optical measuring system

To ease the pre-positioning and alignment of the object under test, a CCD camera with pixel size of about 6 µm X 6 µm is located in the back focal plane of the tube lens to measure the intensity distribution of the reflected light from spherical objects.

3.2 Positioning system

A three-axis positioning stage (NanoMax 303, Thorlabs) with two differential micrometers for x-y axis and a stepper-motor drive for z-axis is employed in the measurement system for pre-adjustment and fine positioning of the object under test.

The two manual micrometers of the stage for lateral positioning feature a resolution of about 1 µm. The achievable z-axis incremental movement resolution with the stepper motor can be up to 60 nm, however the actual repeatability is found to be not better than 0.5 µm. In addition, the cross-talk of this stage for a small positioning range of 500 µm amounts to about 2 µm [8].

3.3 Data evaluation

During the pre-adjustment and fine positioning of the object under test, the lateral position of the focal point of the reflected light on the CCD camera can be determined.

The confocal response of the measurement system close to the interested positions Pos1 and Pos2 of the object under test is acquired by measuring the intensity variation of the reflected light with respect to the z-axis position of the spherical object.

To suppress the negative influence of intensity noise on the measurement signal, correlation analysis technique is proposed to determine the z-axial shift between the confocal curves at Pos1 and Pos2, respectively. Finally, the radius *R* of the sphere under test is defined as the measured relative shift of the two confocal curves.

3.4 Measurement errors

Similar to other confocal microscopes, the actual measurement uncertainty of this optical system suffers from several error sources, including

- intensity fluctuation of the laser light,
- positioning error of the scanning stage,
- high-order form-error and surface roughness of the object under test,
- uncertainty of the correlation analysis, and so on.

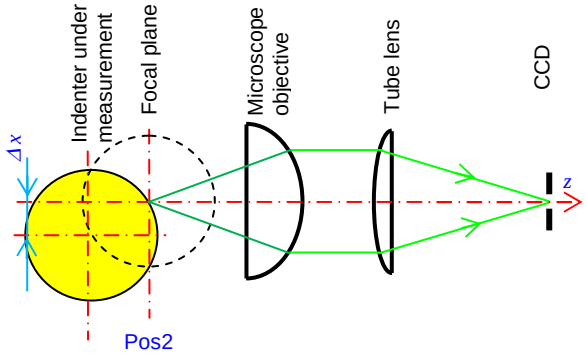

Fig. 3. Analysis of the influence of the stage cross-talk on the measurement errors

Among them, the stage positioning error along the z-axis plays, in general, an import role in error analysis. As for the

influence of the stage lateral distortion Δx, as shown in Fig. 3, in case of Δx << *R*, the measurement error results in

$$\Delta R = \frac{\Delta x^2}{2R}. \qquad (2)$$

Assuming a sphere with *R* = 200 µm under test, and a typical Δx = 2 µm for the stage in use, then a measurement error of 0.01 µm results.

4. EXPERIMENTAL INVESTIGATION

To investigate the actual performance of the optical system, an uncoated spherical sapphire lens with a nominal radius R = 200 µm (shown in Fig. 4) has been measured with the optical setup described above.

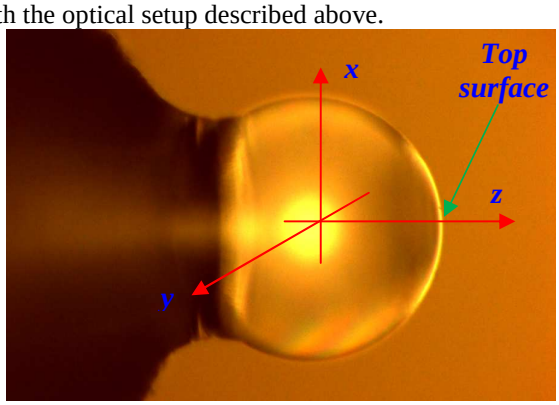

(a) microscopic image of the sapphire sphere glued on a holder

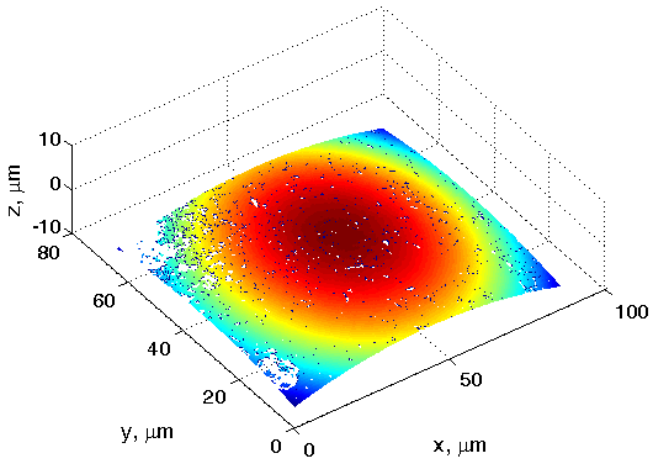

(b) 3-D topography of the spherical lens measured by a confocal microscope

Fig. 4. A sapphire spherical lens used in the experiment and its topography close to its top surface.

The 3D topography of the uncoated sphere has been measured by a commercial confocal microscope, as shown in Fig. 4(b). Of course, due to the limited depth of focus (DOF) of the confocal microscope, the measurable vertical range of the sphere is less than 5 µm. Detailed view to the central region of the top surface of the sphere (as illustrated in Fig. 5) reveals that the sphere has a surface roughness less than 50 nm.

With the help of the 3D-stage mentioned in sub-section 3.2 the sapphire sphere has been scanned. Fig. 6 shows one of the typical position-intensity curves measured when the sphere is moved along the optical axis of the measuring system. To improve the measurement efficiency, fine positioning has been made only within the regions close to the top surface (Pos1) and close to the center of the sphere (Pos2), respectively.

Correlation analysis of the confocal responses close to the top surface and to the sphere center is demonstrated in Fig. 7. It can be seen that the correlation coefficient of the two curves reaches 0.963 when the axial shift of the two confocal responses $\Delta z = z_{Pos2} - z_{Pos1} = 203.59$ µm, and the full-width-half-maximum (FWHM) of the correlation curve amounts to 1.4 µm.

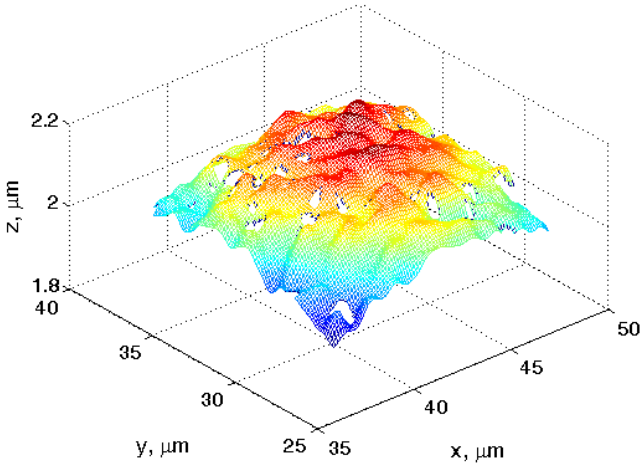

Fig. 5. Topography of the spherical sapphire lens used in the experiment close to the tip top surface measured with a confocal microscope.

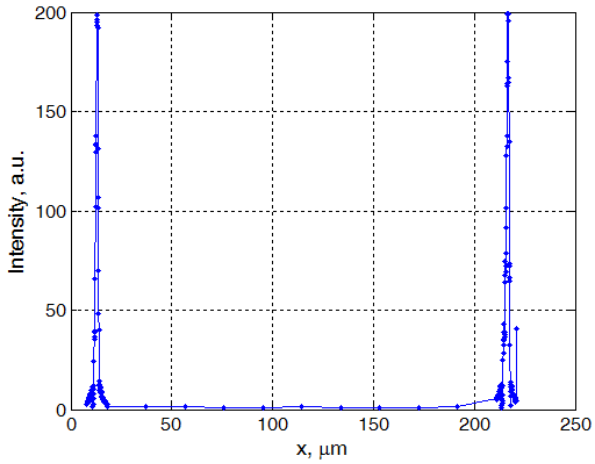

Fig. 6. Typical confocal signal obtained during non-contact scanning of the sapphire sphere shown in Fig. 4(a).

It is interesting to have a detailed look into the confocal signals obtained at z = Pos1 (top surface of the sphere along optical axis) and at z = Pos2 (central plane of the sphere), respectively, as illustrated in Fig. 8. As mentioned above, during the procedure of fine surface scanning, the stepper-motor is moved with a step size of about 80 nm, which

should be larger than the nominal resolution of the 3D-stage. The step-like responses within both of the measured confocal curves reveal that the actual movement resolution of the stage is quite lower than its nominal value.

It can be seen that a nearly perfect confocal response (blue curve with marker "*" in Fig. 8) has been acquired on the sphere top surface, with a FWHM value of about 1.5 µm, indicating a slightly reduced numerical aperture (0.62) due to intentional aperture control of the optical system [6].

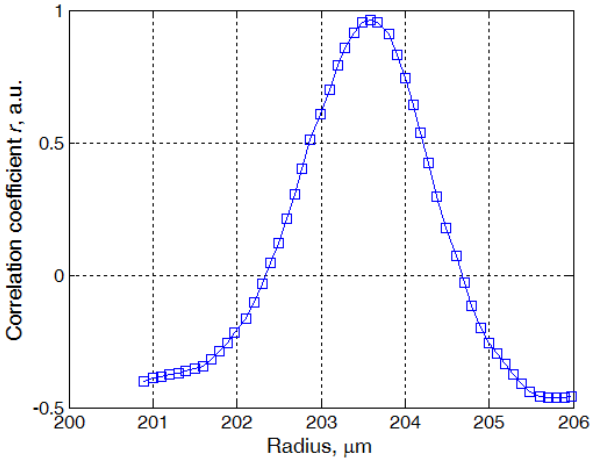

Fig. 7. Determination of the sphere radius by means of correlation analysis of the two confocal responses at the top surface and at the center of the sphere, respectively.

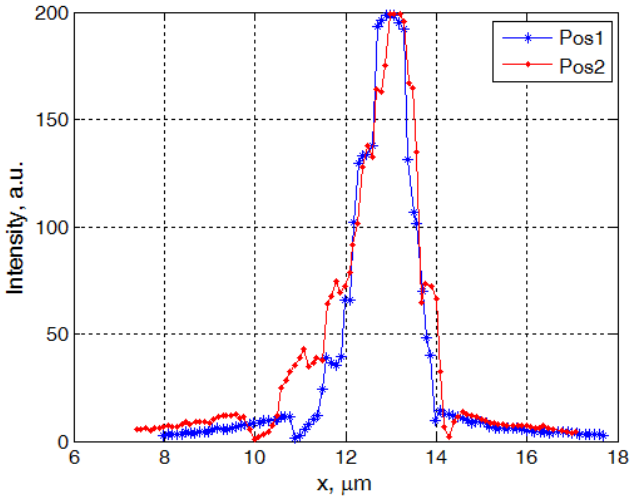

Fig. 8. Comparison of the confocal responses obtained at the top surface of the sphere (z = Pos1) and at the sphere center (z = Pos2), the axial shift between the two curves has been removed.

The confocal response of the sphere close to its center (red curve with the marker "·") demonstrates a FWHM value similar to that of the curve at *z* = Pos1, which means constant resolution of the optical system for a sphere at both measurement positions. Besides this , it's noticeable that the confocal curve at *z* = Pos2 is clearly not symmetric, indicating that the sphere under test should have evidently high-order form errors.

A series of confocal measurements on the sphere shown in Fig. 4(a) has been carried out, and the resulting radii are illustrated in Fig. 9.

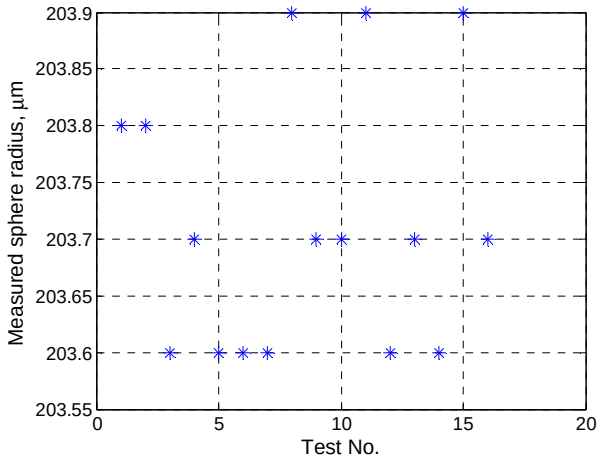

Fig. 9. Repeatability of the developed non-imaging sphere radius measurement system.

From Fig. 9, it can be seen that the measured sphere radius of the sapphire lens has a mean value of 203.7 µm with a repeatability of 0.11 µm.

5. SUMMARY AND OUTLOOK

A practical non-imaging system for the determination of the tip radius of spherical indenters has been presented, which features simple configuration, low cost and high resolution (down to 2.3 µm for normally mounted Rockwell indenters).

The actual performance of the optical setup has been investigated using a sapphire sphere with a nominal radius of 200 µm. A measuring repeatability of 0.11 µm has been achieved with an open-loop stepper-motor drive.

The error sources within the measurement system have been summarized. In addition, detailed analysis of the confocal responses obtained with a sapphire sphere suggests that influence of the high-order form error of the object under test on the radius measurement result should be taken into consideration. This is one of the foci of our work in the near future.

ACKNOWLEDGEMENTS

This research is supported by the European Union by funding the European Metrology Research Programme (EMRP) project "Dynamic Mechanical Properties and Long-term Deformation Behaviour of Viscous Materials" (MeProVisc).

REFERENCES

[1] Pharr G. M., Bolshakov A., "Understanding nanoindentation unloading curves", Journal of Materials Research, 17(10), 2660-71 (2002).

[2] Bouzakis K.-D., Michailidis N., “Coating elastic-plastic properties determined by means of nanoindentations and FEM-supported evaluation algorithms,” Thin Solid Films, 469-470, pp. 227-232, 2004.
[3] ISO 14577, Metallic materials - Instrumented indentation test for hardness and materials parameters, Part 2: Verification and calibration of testing machines, 2002, ISO, Geneva.
[4] Herrmann K., Jennett N.M., Wegener W., Meneve J., Hasche K., Seemann R., “Progress in determination of the area function of indenters used for nanoindentation,” Thin Solid Films, 377/378, pp. 394-400, 2000.
[5] Germak A., Origlia1 C., "Investigations of new possibilities in the calibration of diamond hardness indenters geometry," Measurement, 44(2), pp. 351–358, 2011.
[6] S. Takagi, H. Ishida, T. Usuda, H. Kawachi and K. Hanaki, “Direct Verification and Calibration of Rockwell Diamond Cone Indenters”, Proc. HARDMEKO 2004, pp. 149-154.
[7] Li Z., Gao S., Herrmann K., "An optical microform calibration system for ball-shaped hardness indenters", Proc. SPIE 7718, Optical Micro- and Nanometrology III, 77181C (May 14, 2010).
[8] MAX300 Series NanoMax 3-Axis Flexure Stage, User Guide, Thorlabs, 2010